Underpotential deposition of Cu on Pt(001): Interface structure and the influence of adsorbed bromide

C. A. Lucas
Oliver Lodge Laboratory, Department of Physics, University of Liverpool, Liverpool, L69 7ZE, United Kingdom

N. M. Markovic and P. N. Ross
Materials Sciences Division, Lawrence Berkeley National Laboratory, University of California, Berkeley, California 94720

(Received 10 March 1997; revised manuscript received 17 November 1997)

Using *in situ* x-ray diffraction, we studied the underpotential deposition (UPD) of copper onto a Pt(001) electrode both in pure perchloric acid and in the presence of bromide anions. In pure perchloric acid, the Cu is deposited in pseudomorphic $p(1\times1)$ islands. In the presence of bromide anions, the strong Pt-Br interaction significantly broadens the potential range of Cu UPD. We propose that Br remains in the interface region throughout the UPD process, at first in a disordered Cu-Br phase and then, at more negative potential, forming a $c(2\times2)$ closed-packed monolayer on top of the completed $p(1\times1)$ Cu monolayer. The structures are compared to those found during Cu UPD onto Pt(111), and explained in terms of the metal-halide interactions and the Pt surface atomic geometry. [S0163-1829(98)06120-7]

I. INTRODUCTION

The underpotential deposition (UPD) of a metal onto another metal substrate corresponds to the electrochemical adsorption, often of one monolayer, that occurs at electrode potentials positive of the Nernst potential below which bulk metal adsorption occurs.[1] Numerous experiments have shown that the UPD layer can dramatically alter the chemical and electronic properties of the interface.[2] The UPD layer is also the first stage of bulk metal deposition, and its structure, therefore, can strongly influence the structure of the bulk deposit. Early studies of UPD using polycrystalline substrates[1,3] have, more recently, been extended to single-crystal substrates, which not only allows the role of surface atomic structure to be explored, but also permits a study of the interface structures by diffraction-based techniques, such as low-energy electron diffraction (LEED) and surface x-ray scattering.[4] Many of these studies were performed using emersion methods, whereby the structure formed in an electrochemical cell was transferred into an UHV environment, so that standard surface science probes, such as LEED and Auger electron spectroscopy could be applied.[5] In the past decade, a number of experimental probes, which can study the electrochemical interface *in situ*, have been developed, most notably scanning tunneling microscopy (STM) and synchrotron-based x-ray techniques, adsorption spectroscopy, and surface x-ray diffraction.[4,6,7] These studies have revealed the importance of studying the electrochemical interface *in situ*, where the electrolyte and the strong electric fields at the interface are intact.

As researchers have become more proficient in the use of the *in situ* techniques, a wide range of bimetallic systems have been studied; some examples are Cu/Au(hkl),[8] Tl/Ag(hkl),[9] Pb/Ag(hkl),[10] and Cu/Pt(hkl).[11,12] This has led to a greater understanding of the physics determining the structure of the UPD layer, in particular with regards to the role of the electrode potential and of various other adsorbing species that can be present in solution. In some ways, this development parallels the advances made in UHV studies of metal deposition onto metal substrates, i.e., by molecular-beam epitaxy and other vacuum deposition techniques. The motivation to develop thin metal films with known atomic structures had led to the discovery of a rich variety of physical phenomena, such as surface intermixing and alloying,[13] dealloying,[14] and adsorbate-induced reconstruction.[15] For simple nonalloying systems, the growth mode is dependent on the surface and interface energies, and typically corresponds to one of three cases; layer-by-layer growth (or Frank ver der Merve growth), layer-by-layer growth followed by islanding (Stranski-Krastanov growth) or pure island growth (Volmer-Weber growth).[16] Attempts to tune the growth mode in both homoepitaxial and heteroepitaxial systems has also led to the use of ''surfactants,'' i.e., the presence of another atomic species on the surface to promote a particular growth mode.[17]

In our recent experiments, we have performed a systematic study of the UPD of Cu and Pb onto Pt(111) substrates.[12,18] This was motivated, in part, by the importance of Pt as a catalyst, but also because of the ability to prepare clean ordered Pt surfaces by the technique of flame annealing. This allows fast transfer of the Pt crystal into the electrochemical cell, thus reducing the risk of contamination and eliminating the need for UHV surface preparation.[19] By combining x-ray scattering and rotating ring disk electrode (RRDE) experiments, we were able to propose a detailed mechanism for Cu UPD onto Pt(111). In particular, we showed that halide anions in solution (either chloride or bromide), which form a complete monolayer at positive potentials, remain on the surface throughout Cu UPD, first in an incommensurate 4×4 Cu-halide bilayer structure, and then, at a more negative potential, on top of a pseudomorphic 1×1 Cu monolayer.[18] For contrast we also studied Pb UPD onto Pt(111).[20] In pure perchloric acid, Pb UPD followed a monolayer island growth mode until, at a threshold coverage, a compact $3\times\sqrt{3}$ rectangular structure was formed, as previously reported by Adzic *et al.*[21] The presence of bromide

 © 1998 The American Physical Society

anions in solution had a dramatic influence on the Pb UPD process.[20] Rather than splitting the deposition into a two-stage process, as observed for Cu UPD, the nature of the Pb-Br interaction led to the slow formation of a $p(2\times2)$ structure at the Pt(111) surface which was difficult to stabilize under equilibrium conditions.

In this paper we report a study of the role of surface symmetry in the Cu UPD process by describing x-ray scattering measurements made during Cu UPD onto Pt(001), and comparing the results obtained with similar measurements made on Pt(111). We describe results of Cu UPD in both pure perchloric acid, where there is no strong adsorption of the anion onto the surface, and in perchloric acid containing bromide ions, where there is strong adsorption of the anion onto the surface at all potentials. By combining crystal truncation rod (CTR) measurements with anomalous scattering techniques, we are able to describe both the Cu and Br structures that are formed on the Pt surface during Cu UPD, such as their respective coverages, symmetry, and the Pt-Cu and Cu-Br bond lengths. The results are summarized and compared to those obtained on Pt(111).

II. EXPERIMENTAL DETAILS

The Pt(001) crystal (miscut $\sim0.18°$) was prepared by annealing in a hydrogen flame and cooling in streaming hydrogen before a drop of electrolyte was placed on the surface for transfer into the x-ray electrochemical cell. The x-ray cell was mounted at the center of a four-circle goniometer on beamline 7-2 at the Stanford Synchrotron Radiation Laboratory. X-ray measurements were performed using a focused monochromatic x-ray beam of energy 10 keV (for some measurements the energy was in the range 8.8–9.0 keV, in the region of the Cu K adsorption edge), and defined by slits to be a 0.8×0.8-mm^2 spot at the sample. Diffracted x rays were measured by a Ge solid-state detector after passing through a Soller slit (which defined an in-plane resolution of ~0.005 Å^{-1}) and a 6-mm horizontal slit ~700 mm from the sample. The crystal was indexed to the surface tetragonal unit cell which is related to the conventional cubic unit cell by the transformations $(1,0,0)_t=1/2(2,2,0)_c$, $(0,1,0)_t=1/2(2,-2,0)_c$, and $(0,0,1)_t=(0,0,1)_c$. The spectrometer was aligned using the (0,0,2) and (1,0,1) bulk Bragg reflections.

The electrolyte solution consisted of pyrolytically triply distilled water, 0.1-M $HClO_4$ (EM Science, Suprapur) and 10^{-3}-M Cu^{2+} (from CuO Adrich, Puratronic). To study the effect of bromide anions on the UPD process, 0.01-M KBr (Baker, Ultrex) was added to the electrolyte. The purity of the electrolytes and the cleanliness of the Pt(001) sample after flame annealing were carefully checked by mounting the electrode in a rotating-ring-disk configuration and performing electrochemical measurements.[22] These were in excellent agreement with previous results.[23,24] In the x-ray cell, immediately after mounting in the x-ray goniometer and being put under potential control, the measured cyclic voltammetry (CV) contained all of the main features observed in the electrochemical cell, although with time these features became distorted as the electrolyte made contact with the polycrystalline back and sides of the crystal. After the initial cycling, the electrode potential was transferred to computer control for the duration of the x-ray experiment. All potentials were measured against a Pd/H reference electrode, but are quoted versus a saturated calomel electrode for comparison with previous work.

III. RESULTS

In none of our x-ray scattering experiments of Pt(001) did we observe the vacuum surface reconstruction [hexagonal 5×20 superstructure] (Ref. 25) when the sample is in contact with the electrolyte. We have performed measurements in a number of solutions, e.g., KOH, $HClO_4$, and H_2SO_4, but have always found that the surface is in the unreconstructed 1×1 state at all electrode potentials.[26] The absence of reconstruction was confirmed both by the lack of any superlattice Bragg reflections and by the shape of the specular CTR at positive potential (where no Cu is adsorbed onto the surface). This was similar to the calculation for an ideally terminated 1×1 Pt surface which is shown by the dashed lines in Fig. 2. We have never observed the characteristic shape of the specular CTR associated with the reconstructed surface.[19,27] CV measurements on the Pt(001) surface prepared by flame annealing[28] show features that are consistent with a significant density of atomic steps. In our x-ray scattering experiments, whenever an ordered adlayer superstructure on the Pt(001) surface was observed, the coherent domain size was in the range 30–60 Å [both in this study and in measurements of other adsorbates on the (001) surface]. We propose, therefore, that the flame-annealed Pt(001) surface consists of flat, defect-free terraces of length 30–60 Å separated by adatoms, vacancies, or atomic steps. This contrasts to the flame-annealed Pt(111) surface on which we have observed superstructures with domain sizes of 200–600 Å.[12,18,20] The relatively short terrace lengths on Pt(100) appear to be intrinsic to the hydrogen flame annealing procedure with this crystal face. It should be noted that the measured miscut of 0.18° would give a significantly larger terrace size, ~620 Å for monolayer-high steps. The measured transverse width of the nonspecular CTR, at low l, gave a coherence length which was equal to the resolution of the x-ray spectrometer, and this is consistent with the large terrace size. This implies that additional defects or atomic steps are randomly distributed as observed in STM images of the flame-annealed Pt(001) surface.[29]

A. Cu UPD in 0.1-M $HClO_4$

Changes in the surface structure were monitored during Cu UPD by measuring the scattered intensity at a particular reciprocal-lattice point as the electrode potential was scanned. Such a measurement, at (1,0,0.1), an anti-Bragg position on the non-specular (1,0,l) CTR is shown in Fig. 1(a). Figure 1(b) shows a similar measurement for solution containing 10^{-2}-M KBr, and this will be discussed in Sec. III B. The potential range in Fig. 1(a) was chosen to avoid the region of bulk Cu deposition ($E<-0.2$ V) and the region of surface oxidation and roughening ($E>0.45$ V). The result clearly shows the one-step process that corresponds to Cu deposition (the hysteresis between the anodic and cathodic sweeps being caused by the kinetics of adsorption which depends on the sweep rate, in this case 2 mV/s). Iden-

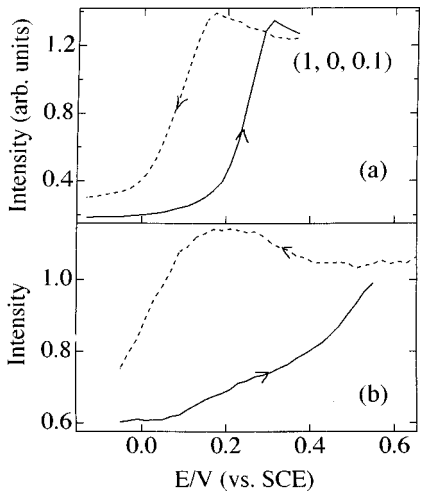

FIG. 1. (a) The measured x-ray intensity at (1,0,0.1) as a function of the electrode potential in solution containing 0.1-M $HClO_4$+10^{-3}-M Cu^{2+}. The solid and dashed lines are for the anodic and cathodic sweep directions, respectively (the sweep rate is 2 mV/s). (b) The measured x-ray intensity at (1,0,0.1) in a solution containing 0.1-M $HClO_4$+10^{-3}-M Cu^{2+}+10^{-2}-M KBr.

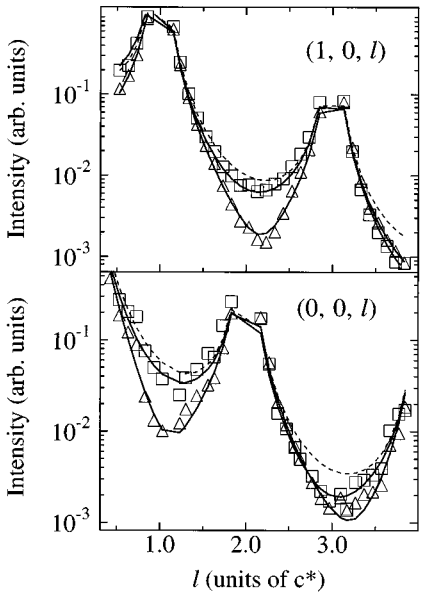

FIG. 2. The crystal truncation rods (CTR's) measured at an electrode potential of −0.13 V (triangles) and 0.14 V (squares) in 0.1-M $HClO_4$+10^{-3}-M Cu^{2+}. The dashed lines are calculations for an ideally terminated Pt(001) surface, and the solid lines are the best fits to the data according to the structural model described in the text and the parameters listed in Table I.

tical results to that of Fig. 1(a) were obtained at (0,0,1.03), a position on the specular CTR which is insensitive to the in-plane order of the Cu adlayer. The exact matching between the specular and nonspecular CTR results implies that the adsorbed Cu is ordered in commensurate Pt sites, probably the fourfold hollow site, as this would cause the observed decrease at (1,0,0.1). Holding the electrode potential at −0.13 V, the negative potential limit, we searched for superlattice diffraction peaks by scanning along the ⟨1,0,0⟩ and ⟨1,1,0⟩ directions, at $l=0.1$, and then repeated the measurement after stepping the electrode potential to 0.19 V, just before the onset of complete Cu desorption from the surface. In both cases we observed no additional diffraction peaks other than those from the Pt(001) surface, and so we conclude that Cu is deposited into a $p(1\times1)$ pseudomorphic overlayer.

In the absence of superlattice reflections, structural information about the Cu adlayer can be obtained by modeling of the CTR data. The data measured at −0.13 V for the $(0,0,l)$ and $(1,0,l)$ CTR's are shown in Fig. 2. To model the data we included a partial coverage θ_{Cu} of Cu adatoms in fourfold hollow sites on the Pt(001) surface lattice, and allowed the coverage, the surface normal spacing $d_{Pt\text{-}Cu}$, and the Debye-Waller-type roughness,[30] σ_{Cu}, of the Cu layer to vary (full details of the scattering equations are described in Refs. 19 and 31). The best fit is shown by the solid lines in Fig. 2 according to the structural parameters listed in Table I. The surface roughness of the Pt substrate, σ_{Pt}, was fixed at the value determined by fits to nonspecular CTR data measured at 0.4 V, where no Cu is adsorbed onto the electrode surface (i.e., fitted with a single parameter). The dashed lines in Fig. 2 are a calculation of the scattering from an ideally terminated Pt(001) lattice. Clearly, the simple structural model we use is capable of describing the data. Also listed in Table I are the parameters derived from a fit to similar data measured at 0.19 V. These data and best fit are also shown in Fig. 2, which confirms that the kinetic measurements in Fig. 1(a) are repeated under steady-state or equilibrium conditions. We note that the intensity changes shown in Fig. 1(a) and the data in Fig. 2 indicate that at positive potential the CTR data were similar to that of the ideal 1×1 surface (dashed lines in Fig. 2). Given that the changes in the x-ray data, which are fully reversible with potential, correlate with the Cu UPD features which are well known from cyclic voltammetric studies, it is apparent that the x-ray data are sensitive to the deposition of Cu, and not simply roughening of the Pt surface. This was confirmed by varying the incident x-ray energy in the region of the Cu K adsorption edge. At positions on the CTR's where the Cu contribution to the scattered intensity was relatively large, i.e., midway between the Bragg reflections, the scattered intensity showed the expected energy dependence across the Cu K edge. A detailed set of measurements in which this technique is further exploited is presented in Sec. III B.

According to a hard-sphere model and using the metallic radii of Pt (1.39 Å) and Cu (1.28 Å), a vertical spacing of 1.81 Å for Cu adsorbed into a Pt(001) fourfold hollow site is calculated. This is in excellent agreement with the value we

TABLE I. Parameters used to calculate the solid lines in Fig. 2. The Pt surface roughness was fixed at the value determined at positive potential (where no Cu is adsorbed onto the surface) from a single parameter fit to the nonspecular CTR.

	Electrode potential	
	−0.13 V	+0.19 V
σ_{Pt}	0.1±0.05 Å	0.1±0.05 Å
θ_{Cu} (per Pt surface atom)	0.8±0.1	0.18±0.1
$d_{Pt\text{-}Cu}$	1.84±0.07 Å	1.88±0.09 Å
σ_{Cu}	0.10±0.1 Å	0.15±0.1 Å

obtained from our fit to the CTR data. It appears, therefore, that Cu grows as 1×1 pseudomorphic islands on the Pt(001) surface and reaches a coverage of 0.80 ML at -0.13 V. By stepping the electrode potential more negatively, it may be possible to complete the Cu monolayer. At 0.19 V, a potential where the Cu is partially desorbed, we obtained a coverage of 0.18 ML. At this potential we were unable to observe any superlattice diffraction pattern, for example, from a $c(2\times2)$ structure. Our results are in good agreement with the *ex situ* LEED study by Aberdam *et al.*,[32] in which it was also suggested that Cu was deposited into $p(1\times1)$ pseudomorphic islands. We can find no evidence of the $c(2\times2)$ structure that was proposed in Ref. 23 to be formed in the first stages of Cu deposition. The sharp change in intensity at (1,0,0.1) [Fig. 1(a)] indicates that Cu deposition occurs as pseudomorphic island growth and is not a two-step process.

B. Cu UPD in 0.1-M $HClO_4$+0.01-M KBr

In a previous publication we described RRDE and x-ray scattering measurements of bromide adsorption onto Pt(001) in 0.1-M $HClO_4$.[33] Briefly, the results showed that bromide adsorption began at an electrode potential of ~-0.25 V, and reached a coverage θ_{Br} of ~0.42 ML at 0.5 V. Although we were unable to detect any in-plane superlattice peaks corresponding to long-range order in the Br adlayer, CTR measurements implied that Br formed a strong covalent bond with the Pt substrate, and was probably present in a mixture of short-range ordered structures which covered the Pt(001) surface. This conclusion was also suggested on the basis of STM results.[29]

The effect of bromide adsorbed onto the surface on the Cu UPD process is illustrated in Fig. 1(b), which shows the measured x-ray intensity at (1,0,0.1) as a function of the electrode potential. Comparison with Fig. 1(a) indicates that the adsorbed bromide broadens the potential range of Cu deposition, but there is no evidence of a stagewise deposition process. This contrasts with results obtained on the Pt(111) surface (see Fig. 1 of Ref. 12), where two distinct steps in Cu UPD were observed, the first corresponding to formation of a Cu-Br bilayer with Cu bonded to Pt and Br in the topmost atomic layer. There is a larger hysteresis in the x-ray intensity at (1,0,0.1) in the presence of adsorbed Br, indicative of the slower kinetics of ordering of Cu adatoms into the pseudomorphic structure. This effect may arise from the stronger Pt-Br interaction on the (001) surface, which induces competition between Cu and Br for the Pt adsorption sites, and broadens the potential range of Cu UPD.

We held the electrode potential at 0.43, 0.12, and -0.13 V, in each case allowing enough time for the system to reach an equilibrium state, and then searched for in-plane scattering peaks. The search consisted of scans along the high-symmetry, in-plane Pt reciprocal-lattice directions at $l=0.1$, and rotational scans at positions where incommensurate adlayers would be expected to give scattered intensity, e.g., at $Q=|100|_{Br}$ and $Q=|100|_{Cu}$. In agreement with our previous work, we found no peaks at 0.43 V, where only Br is adsorbed onto the surface.[33] In addition, no peaks were found at 0.12 V, an intermediate potential where, on the Pt(111) surface under identical conditions, we observed a structure with approximately 4×4 symmetry that corresponded to an incommensurate Cu-Br bilayer.[12,18] At -0.13 V, however, we observed peaks at reciprocal-lattice positions which could be indexed to a $c(2\times2)$ structure. The in-plane scattering in reciprocal space is represented in Fig. 3, together with some rocking scans at the various reciprocal-lattice points that are indicated (a) $(\frac{1}{2},\frac{1}{2},0.1)$, (b) (0,1,0.1), and (c) $(\frac{1}{2},\frac{3}{2},0.1)$. No peaks were observed at any reciprocal-lattice points with higher symmetry than the $c(2\times2)$ structure, such as those expected for a $c(\sqrt{2}\times2\sqrt{2})R45°$ structure,[34] which also gives rise to Bragg reflections at the positions defined by the $c(2\times2)$ unit cell. As can be seen from Fig. 3, all of the measured $c(2\times2)$ reflections were relatively broad compared to the peak at (1,0,0.1) on the Pt CTR and, from Lorentzian fits to the data (solid lines in Fig. 3), a domain size in the range 30–60 Å for the $c(2\times2)$ structure was calculated.[35] As mentioned earlier, we believe that 30–60 Å is the range of terrace sizes on the flame-annealed Pt(001) surface in between atomic steps and defects. No dependence of the measured domain size on the potential sweep rate was observed. The $c(2\times2)$ diffraction pattern was, however, only formed if the electrode potential was held in the region below -0.12 V and, even then, only if the potential was approached from a more negative potential. Once formed, the $c(2\times2)$ structure was stable at negative potential, until the onset of bulk Cu deposition.

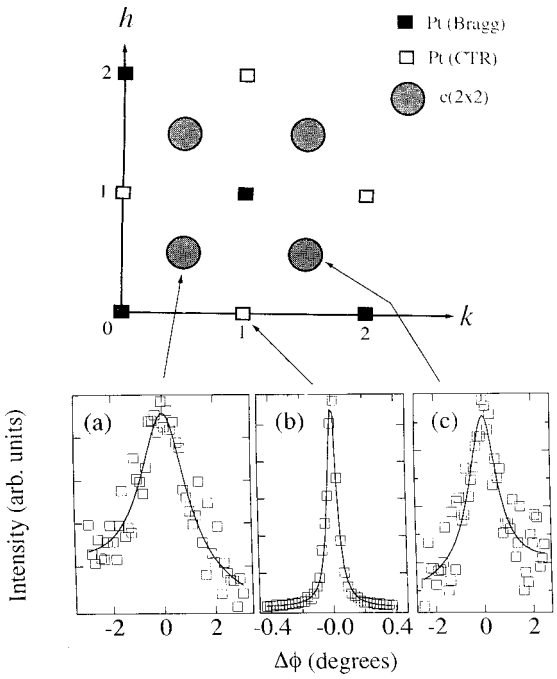

FIG. 3. A representation of the in-plane scattering measured at -0.13 V in solution containing 0.1-M $HClO_4$+10^{-3}-M Cu^{2+} +10^{-2}-M KBr. The solid circles correspond to the measured $c(2\times2)$ reflections and the squares to the location of bulk Pt CTR's and Pt Bragg reflections. The lower figures show scans through the indicated reciprocal lattice points at (a) $(\frac{1}{2},\frac{1}{2},0.1)$, (b) (0,1,0.1), and (c) $(\frac{1}{2},\frac{3}{2},0.1)$. In each case the solid lines are fits of a Lorentzian line shape to the data.

In our previous study of Cu UPD onto Pt(111), we used anomalous scattering techniques to show that the 4×4 structure observed in the first stage of Cu deposition contained both Cu and Br in the unit cell.[12] This was determined by measuring the integrated intensities of the 4×4 superlattice

reflections, as the incident x-ray energy was tuned close to the Cu *K* adsorption edge (8979 eV). Systematic changes in the measured intensities were used to derive a structural model. Given that the $c(2\times2)$ diffraction pattern in this study was obtained at -0.13 V, a potential where a significant amount of Cu is adsorbed onto the surface, we performed similar measurements at several l values along the $(\frac{1}{2},\frac{1}{2},l)$ and $(\frac{1}{2},\frac{3}{2},l)$ rods (the intensity along these rods showed a gradual decrease as a function of l, although their exact form was complicated by adsorption of x rays by the trapped electrolyte at low-l values). Measurements of the integrated intensities at 8779 and 200 eV below the Cu *K* adsorption edge, and 8974 and 5 eV below the Cu edge, were performed, but showed absolutely *no dependence* on the incident x-ray energy. Given that the dispersion corrections to the Cu atomic form factor change significantly over this energy range,[36] this result implies that no Cu is contained in the $c(2\times2)$ unit cell. It seems likely, therefore, that the $c(2\times2)$ structure consists of an ordered Br lattice which is formed on top of a pseudomorphic Cu layer.

The intensity distribution of the $c(2\times2)$ reflections was very simple, showing a Q-dependent decrease that was slightly more rapid than calculated for a perfect structure, presumably due to disorder. To obtain more detailed structural information, we again used CTR measurements, as in Sec. II, modifying the scattering equations to include a $c(2\times2)$ Br adlayer on top of a $p(1\times1)$ pseudomorphic Cu monolayer and allowing the respective coverages, surface normal spacings, and roughnesses to vary in order to fit the data. The CTR's passing through the bulk Pt Bragg reflections include contributions to the scattering both from the Cu and Br adlayers and the Pt lattice. In modeling of CTR data, there is always some question as to the uniqueness of the model that is used for the starting point for structural refinement. To further test the model, we measured the CTR's with incident x-ray energies of 8779 and 8974 eV, and simultaneously refined the structural parameters to fit both the raw CTR data set (measured at 10 keV) and the intensity ratio $I_{8779\,\mathrm{eV}}/I_{8974\,\mathrm{eV}}$. This method increases the sensitivity of the fitting procedure to the Cu layer as changes in the Cu atomic form factor are known from calculations of the dispersion corrections.[36] We previously used this method to determine accurately the Cu coverage during Cu UPD onto Pt(111) in the presence of sulfate anions.[37]

CTR data taken with the potential held at -0.13 V, where the $c(2\times2)$ structure was present, is shown in the lower panels of Fig. 4. Comparison of these data with Fig. 2 shows that the increased thickness of the adsorbed structure leads to the oscillation in between the bulk Bragg reflections (this is most noticeable in between $l=0$ and $l=2$ on the specular CTR). The top panels in Fig. 4 show the ratio data sets $I_{8779\,\mathrm{eV}}/I_{8974\,\mathrm{eV}}$, which clearly indicates the sensitivity of the CTR measurements to the Cu adlayer. The solid lines in Fig. 4 correspond to the results of a simultaneous fit to these data sets in which the Cu coverage θ_{Cu}, Pt-Cu spacing $d_{\mathrm{Pt\text{-}Cu}}$, coverage of Br in a $c(2\times2)$ adlayer, i.e., two Br atoms per $c(2\times2)$ unit cell θ_{Br}, Cu-Br spacing $d_{\mathrm{Cu\text{-}Br}}$, and the Cu and Br roughnesses were varied. The results are listed in Table II. A schematic of the structure is shown in Fig. 5. Although measurement of the (1,0,l) CTR does not rule out the possibility of adsorption into twofold bridge sites, this is unlikely because of the derived bond lengths (see Table II). Also, Fig. 6 shows the measured (1,1,l) CTR together with calculated profiles using the parameters in Table II for the Cu-Br overlayer structure being adsorbed at Pt twofold bridge sites (dashed line) and fourfold hollow sites (solid line). Clearly, this supports the assignment of the fourfold hollow site.

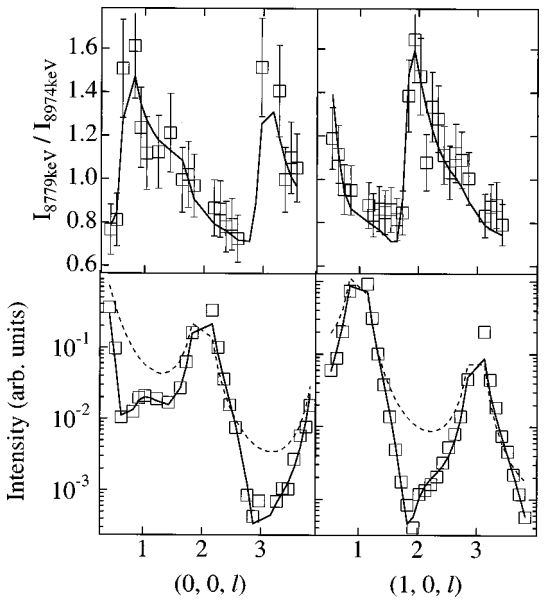

FIG. 4. (Lower panels) the measured CTR's at an electrode potential of -0.13 V in 0.1-M $HClO_4$+10^{-3}-M Cu^{2+}+10^{-2}-M KBr, where the $c(2\times2)$ structure is present. (Upper panels) the ratio between CTR data sets taken with incident x-ray photon energies of 8779 and 8974 eV, i.e., $I_{8779\mathrm{eV}}/I_{8974\mathrm{eV}}$. The solid lines are results of a simultaneous fit to all of the data according to the structural model which is schematically illustrated in Fig. 5, and the parameters listed in Table II.

Although the presence of Br anions considerably slows the kinetics of ordering, at negative potential (-0.13 V) a complete pseudomorphic $p(1\times1)$ Cu monolayer is formed on the Pt(001) surface. When this monolayer is completed, Br forms a $c(2\times2)$ overlayer on top of the Cu monolayer. The Cu-Br spacing implies that, as was the case for the Pt-Br bond for Br adsorption onto Pt(001),[33] the metal-halide bond is covalent in nature. The near-neighbor spacing in the Br adlayer is 3.92 Å, which is similar to the near-neighbor spacing of Br adsorbed onto Pt(111) at positive electrode potential.[38] The Br coverage on the pseudomorphic Cu monolayer is nearly identical to the coverage measured on

TABLE II. Structural parameters to the fit to the data in Fig. 4. The coverages θ_{Cu} and θ_{Br}, are with respect to a full copper monolayer (one Cu atom per surface Pt atom) and a full $c(2\times2)$ Br adlayer (0.5 Br atoms per surface Pt atom).

θ_{Cu}	1.0 ± 0.06
$d_{\mathrm{Pt\text{-}Cu}}$	1.75 ± 0.05 Å
σ_{Cu}	0.13 ± 0.05 Å
$\theta_{\mathrm{Br}}[c(2\times2)]$	0.9 ± 0.1
$d_{\mathrm{Cu\text{-}Br}}$	1.79 ± 0.08 Å
σ_{Br}	0.3 ± 0.2 Å

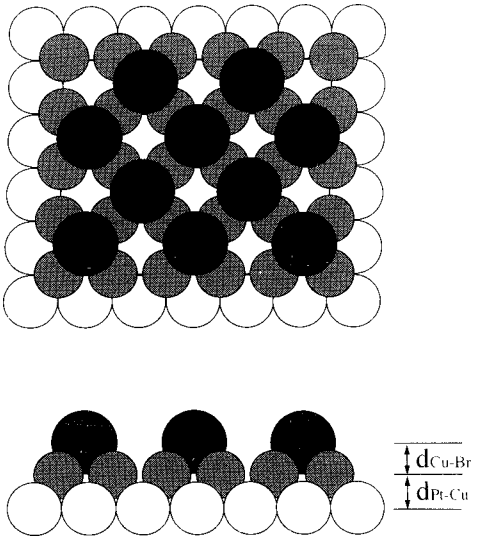

FIG. 5. Top and side view representations of the proposed $c(2\times2)$ structure observed at -0.13 V. The open circles are Pt substrate atoms, the shaded circles are Cu atoms, and the black circles are Br atoms which form the $c(2\times2)$ structure. The side view indicates the surface normal spacings listed in Table II that are derived from the CTR measurements shown in Fig. 4.

the Pt surface at positive potential, and implies that close to a full Br monolayer remains on the electrode surface during Cu UPD. It is interesting that the bromide layer forms a structure with long-range order on the Cu monolayer and not on the Pt(001) surface in a solution free of Cu.[33]

IV. DISCUSSION

In pure perchloric acid, Cu is deposited as $p(1\times1)$ islands on the Pt(001) surface. The islands probably nucleate at step edges. Due to the size of the Cu adatom, adsorption at step edges can occur at the overcoordinated fourfold hollow Pt sites, which then nucleates growth as a pseudomorphic adlayer due to the mobility of the Cu adatom on the Pt terrace and the Cu-Cu interaction. A similar mechanism of Cu growth on Pt(001) was observed in UHV deposition studies[39] and in an *ex situ* LEED study of Cu UPD.[32]

When bromide is adsorbed onto Pt(001) in the solution free of Cu^{2+}, no structure with long-range order is observed,[29,33] in contrast to the ordered hexagonal incommensurate structures observed on Pt(111).[38,40] The size of the Br adatoms (they are completely discharged[33]), the symmetries of the orbitals participating in the covalent bond, and the differences in both the symmetries and corrugation of the two substrates, are all contributing factors. Preferential adsorption at step sites may also be responsible for the short-range order in the Br adlayer.

In the solution containing Cu^{2+} and Br^-, at potentials positive of ~0.4 V, the Pt surface is covered with adsorbed Br to the same coverage as in the solution free of Cu^{2+}. As the electrode potential is swept negatively from 0.4 V, there is a increasing thermodynamic driving force for Cu cations to displace the adsorbed Br from the Pt adsorption sites. While the details of charge transfer and Cu-Br place exchange remain unknown, it is established that on Pt(111) this is a two-stage process with the formation of a Cu-Br bilayer intermediate phase. On Pt(001), in the intermediate potential range (0.1–0.4 V) of submonolayer Cu coverage, we could determine only that a mixture of Cu and Br atoms is present on the Pt(001) surface in a disordered structure. Presumably the strong affinity of adsorbates for the Pt fourfold hollow site prevents the formation of a long-range ordered bilayer phase [for example, a (001) plane of Cu(I)Br] as adsorbate mobility is reduced on the (001) substrate.

As with Pt(111), we propose that the Br remains adsorbed on the electrode throughout the deposition process, having essentially the same coverage (possibly even slightly higher) on the Cu monolayer as on the Cu-free Pt(001) surface (at positive potentials). In contrast to the Pt(111) surface, however, where no ordered Br structures on top of the Cu monolayer were observed, the Br forms a commensurate overlayer structure, a $c(2\times2)$-Br adlattice on the $p(1\times1)$-Cu lattice (Fig. 5). The simplest explanation we can offer for this difference in ordering can be seen in the structural models of Fig. 5. The fourfold hollow sites are deeper (by ~0.1 Å) in the (001)-$p(1\times1)$-Cu structure than the threefold hollow sites in the P(111)-$p(1\times1)$-Cu structure, meaning that the Br adatoms would sit in deeper potential wells on the (001)-$p(1\times1)$-Cu surface. This favors the formation of a commensurate $c(2\times2)$ phase. In addition to the surface corrugation factor, there are also differences in Pt-Cu-Br chemical bonding between the two symmetries that may be even more important. The effective radii of Cu and Br in the structure in Fig. 5 can be calculated from the interplanar spacings in Table II, 1.24 and 1.35 Å, respectively. Since the covalent radius of Br is 1.14 Å, and the atomic radius of bulk Cu is 1.28 Å, the experimental radii indicate strong bonding with some ionic character, e.g., $Cu^{+\delta}$–$Br^{-\delta}$. The symmetries of the orbitals participating in this bonding may favor ordering in the square lattice of the (001) surface, and not the hexagonal lattice of the (111) surface.

Finally, we note that our results have interesting consequences for the metal multilayer growth regime, in particular with regard to the presence of the adsorbed Br adlayer. The presence of other adsorbing species in the solution, and the fact that these species are influenced by the strong electric

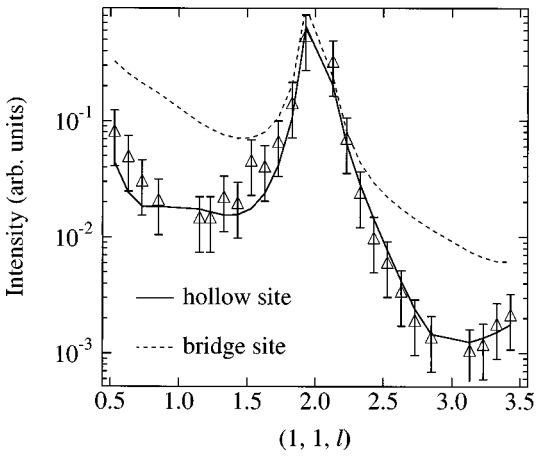

FIG. 6. The (1,1,l) CTR measured at -0.13 V, where the $c(2\times2)$ structure was present. The dashed line and solid line are calculated from the parameters in Table II for the Cu Br-$c(2\times2)$ structure, being anchored at Pt twofold bridge sites and Pt fourfold hollow sites, respectively.

field at the interface, are the major differences between UHV studies of metal deposition and electrodeposition. The mechanism by which the adsorbed Br monolayer remains at, or near, the interface during deposition of a Cu monolayer is unique to the electrochemical environment. Taking this a stage further, and given the strong nature of the Cu-Br interaction, it is evident that the bromide layer participates in the early stages of multilayer Cu deposition, and may act as a kind of surfactant in the epitaxial growth. Indeed, the $c(2\times2)$ Br adlayer remained on the surface as the potential was decreased to the onset of bulk Cu deposition. In these solutions, however, the kinetics of bulk Cu deposition were rather fast and, although some differences were observed between multilayer Cu deposition in pure perchloric acid and in the presence of bromide, it was difficult to quantify the changes.[41] Further experiments are in progress to study the multilayer growth mechanism.

ACKNOWLEDGMENTS

We would like to thank Frank Zucca for his technical support, and the staff and user administration at the Stanford Synchrotron Radiation Laboratory (SSRL) for providing an excellent facility. Sean Brennan is thanked both for his support of beamline 7-2 and for supplying us with the computer codes for calculation of the dispersion corrections. This work was supported by the Director, Office of Energy Research, Materials Science Division (MSD) of the U.S. Department of Energy (DOE) under Contract No. DE-AC03-76SF00098. Research was carried out in part at SSRL, which is funded by the Division of Chemical Sciences (DCS), U.S. DOE.

[1] D. M. Kolb, in *Advances in Electrochemistry and Electrochemical Engineering*, edited by H. Gerischer and C. Tobias (Wiley, New York, 1978), Vol. 11.

[2] R. R. Adzic, in *Advances in Electrochemistry and Electrochemical Engineering*, edited by H. Gerischer (Wiley, New York, 1984), Vol. 13.

[3] D. M. Kolb, M. Przasnyski, and H. Gerischer, J. Electroanal. Chem. **54**, 25 (1974).

[4] For a recent review, see A. J. Bard *et al.*, J. Phys. Chem. **97**, 7147 (1993).

[5] A. T. Hubbard, Chem. Rev. **88**, 633 (1988).

[6] See papers in *Proceedings of the IUVSTA Workshop on Surface Science and Electrochemistry* [Surf. Sci. **335**, 1 (1995)].

[7] For review articles, see M. F. Toney and B. M. Ocko, Synch. Radiat. News **6**, 28 (1993); M. F. Toney and O. R. Melroy, in *Electrochemical Interfaces: Modern Techniques for In-Situ Interface Characterization*, edited by H. Abruna (VCH Verlag, Berlin, 1991), p. 57.

[8] O. M. Magnussen, J. Hotlos, R. J. Nichols, D. M. Kolb, and R. J. Behm, Phys. Rev. Lett. **64**, 2929 (1990), M. F. Toney, J. N. Howard, J. Richer, G. L. Borges, J. G. Gordon, O. R. Melroy, D. Yee, and L. B. Sorensen, *ibid.* **75**, 4472 (1995).

[9] M. F. Toney, J. G. Gordon, M. G. Samant, G. L. Borges, O. R. Melroy, L.-S. Kau, D. G. Wiesler, D. Yee, and L. B. Sorensen, Phys. Rev. B **42**, 5594 (1990); M. F. Toney, J. G. Gordon, M. G. Samant, G. L. Borges, O. R. Melroy, D. Yee, and L. B. Sorensen, *ibid.* **45**, 9362 (1992); J. X. Wang, R. R. Adzic, O. M. Magnussen, and B. M. Ocko, Surf. Sci. **344**, 111 (1995).

[10] O. R. Melroy, M. F. Toney, G. L. Borges, M. G. Samant, J. G. Gordon, L.-S. Kau, D. G. Wiesler, J. Kortright, P. N. Ross, D. Yee, and L. B. Sorensen, Phys. Rev. B **38**, 10 962 (1988); W. Obretenov, U. Schmidt, W. J. Lorenz, G. Staikov, E. Budveski, D. Carnal, U. Muller, H. Siegenthaler, and E. Schmidt, J. Electrochem. Soc. **140**, 692 (1992).

[11] H. S. Yee and H. D. Abruna, J. Phys. Chem. **97**, 6278 (1993); H. Matsumoto, J. Inukai, and M. Ito, J. Electronanal. Chem. **379**, 223 (1994); G. Beiter, O. M. Magnussen, and R. J. Behm, Surf. Sci. **336**, 19 (1995).

[12] I. M. Tidswell, C. A. Lucas, N. M. Markovic, and P. N. Ross, Phys. Rev. B **51**, 10 205 (1995).

[13] C. Stampfl, M. Scheffler, H. Over, J. Burchhardt, M. Nielsen, D. L. Adams, and W. Moritz, Phys. Rev. Lett. **69**, 1532 (1992); S. Rousset, S. Chiang, D. E. Fowler, and D. D. Chambliss, *ibid.* **69**, 3200 (1992); J. Neugebauer and M. Scheffler, *ibid.* **71**, 577 (1993); L. P. Nielsen, F. Besenbacher, I. Stensgaard, E. Laegsgaard, C. Engdahl, P. Stolze, K. W. Jacobsen, and J. K. Norskov, *ibid.* **71**, 754 (1993); H. Roder, R. Schuster, H. Brune, and K. Kern, *ibid.* **71**, 2086 (1993).

[14] L. P. Nielsen, F. Besenbacher, I. Stensgaard, E. Laegsgaard, C. Engdahl, P. Stolze, and J. K. Norskov, Phys. Rev. Lett. **74**, 1159 (1995); Y. G. Shen, J. Yao, D. J. O'Connor, B. V. King, and R. J. MacDonald, J. Phys.: Condens. Matter **8**, 4903 (1996).

[15] B. E. Hayden, K. C. Prince, P. J. Davie, G. Paolucci, and A. M. Bradshaw, Solid State Commun. **48**, 325 (1983); C. J. Barnes, M. Q. Ding, M. Lindous, R. D. Diehl, and D. A. King, Surf. Sci. **162**, 59 (1985); J. W. M. Frenken, R. L. Krans, J. V. van der Veen, E. Holub-Krappe, and K. Horn, Phys. Rev. Lett. **59**, 2307 (1987); C. L. Fu and K. M. Ho, Phys. Rev. Lett. **63**, 1617 (1989).

[16] For a review, see E. Bauer, Appl. Surf. Sci. **11/12**, 479 (1980).

[17] H. A. van der Vegt, J. M. C. Thornton, H. M. van Pinxteren, M. Lohmeier, and E. Vlieg, Phys. Rev. Lett. **68**, 3335 (1992); G. Rosenfeld, R. Servaty, C. Teichert, B. Poelsema, and G. Comsa, *ibid.* **71**, 895 (1993); J. Vrijmoeth, H. A. van der Vegt, J. A. Meyer, E. Vlieg, and R. J. Behm, *ibid.* **72**, 3843 (1994).

[18] N. M. Markovic, H. A. Gasteiger, C. A. Lucas, I. M. Tidswell, and P. N. Ross, Surf. Sci. **335**, 91 (1995); C. A. Lucas, N. M. Markovic, I. M. Tidswell, and P. N. Ross, Physica B **221**, 245 (1996); N. M. Markovic, C. A. Lucas, H. A. Gasteiger, and P. N. Ross, Surf. Sci. **372**, 239 (1997).

[19] I. M. Tidswell, N. M. Markovic, C. A. Lucas, and P. N. Ross, Phys. Rev. B **47**, 16 542 (1992); I. M. Tidswell, N. M. Markovic, and P. N. Ross, Phys. Rev. Lett. **71**, 1601 (1993).

[20] N. M. Markovic, B. N. Grgur, C. A. Lucas, and P. N. Ross, J. Electroanal. Chem. (to be published). At present we do not have a definitive structural model for the $p(2\times2)$ structure.

[21] R. R. Adzic, J. Wang, C. M. Vitus, and B. M. Ocko, Surf. Sci. **293**, L876 (1993).

[22] For more details of the RRDE technique, see N. M. Markovic, H. A. Gasteiger, and P. N. Ross, Langmuir **11**, 4098 (1995).

[23] D. M. Kolb, R. Koetz, and K. Yama, Surf. Sci. **87**, 20 (1979).

[24] C. L. Scortichini and C. N. Reilley, J. Electroanal. Chem. **139**, 233 (1982); P. C. Andricacos and P. N. Ross, *ibid.* **167**, 301

(1984); N. M. Markovic and P. N. Ross, Langmuir **9**, 580 (1993).

[25] For some recent studies, see D. L. Abernathy, S. G. J. Mochrie, D. M. Zehner, G. Grübel, and D. Gibbs, Phys. Rev. B **45**, 9272 (1992); K. Kuhnke, K. Kern, G. Comsa, and W. Moritz, *ibid.* **45**, 14 388 (1992).

[26] Recently, some remnants of the Pt(001) reconstruction have been observed by STM after contact with electrolyte, M. S. Zei, N. Batina, and D. M. Kolb, Surf. Sci. **306**, L519 (1994).

[27] D. L. Abernathy, S. G. J. Mochrie, D. M. Zehner, G. Grubel, and D. Gibbs, Phys. Rev. Lett. **69**, 941 (1992).

[28] N. M. Markovic and P. N. Ross, J. Electroanal. Chem. **330**, 499 (1992), and references therein.

[29] A. M. Bittner, J. Wintterlin, B. Beran, and G. Ertl, Surf. Sci. **335**, 291 (1995).

[30] Included in addition to the thermal Debye-Waller factor (which was fixed at the bulk values for Pt, Cu, and Br) by multiplying each scattering amplitude by $\exp(-q^2\sigma^2/2)$, where q is the surface normal momentum transfer and σ is the surface normal displacement amplitude. See Ref. 9 and J. Wang, B. M. Ocko, A. J. Davenport, and H. S. Isaacs, Phys. Rev. B **46**, 10 321 (1992) for more details.

[31] B. M. Ocko, D. Gibbs, K. G. Huang, D. M. Zehner, and S. G. J. Mochrie, Phys. Rev. B **44**, 6429 (1991).

[32] D. Aberdam, Y. Gauthier, R. Durand, and R. Faure, Surf. Sci. **306**, 114 (1994).

[33] N. M. Markovic, C. A. Lucas, H. A. Gasteiger, and P. N. Ross, Surf. Sci. **365**, 229 (1996).

[34] B. M. Ocko, O. M. Magnussen, J. X. Wang, and T. Wandlowski, Phys. Rev. B **53**, R7654 (1996).

[35] Calculated as domain size, $D=2/\Delta Q$, where ΔQ is the FWHM of the peak in Å^{-1}.

[36] f' changes from -3.4 electrons to -7.3 electrons, calculated from S. Brennan and P. L. Cowan, Rev. Sci. Instrum. **63**, 850 (1992).

[37] C. A. Lucas, N. M. Markovic, and P. N. Ross, Phys. Rev. B **56**, 3651 (1997).

[38] C. A. Lucas, N. M. Markovic, and P. N. Ross, Surf. Sci. **340**, L949 (1995).

[39] C. J. Barnes, M. Lindroos, and M. Pessa, Surf. Sci. **152/153**, 260 (1985); Y. S. Li, J. Quinn, H. Li, D. Tian, F. Jona, and P. M. Marcus, Phys. Rev. B **44**, 8261 (1991).

[40] C. A. Lucas, N. M. Markovic, and P. N. Ross, Phys. Rev. B **55**, 7964 (1997).

[41] There was some indication that bromide promoted a layer-by-layer growth mode as evidenced by periodic oscillations in the x-ray intensity measured at selected reciprocal lattice points on the CTR's after the potential was stepped into the bulk Cu deposition regime [C. A. Lucas, N. M. Markovic, and P. N. Ross (unpublished)].